TIME-FREQUENCY PARAMETERIZATION OF DOUBLY DISPERSIVE CHANNELS

Ziyang Ju, Thomas Hunziker, and Dirk Dahlhaus

Communications Laboratory, University of Kassel
Wilhelmshöher Allee 73, D-34121, Kassel, Germany
phone: +49 561 804-6557, fax: +49 561 804-6008, email: {ju,hunziker,dahlhaus}@uni-kassel.de
web: www.comlab.uni-kassel.de

ABSTRACT

We propose a new approach for describing doubly dispersive discrete-time channels based on concepts from Gabor analysis. The channel input is mapped onto the output via time-frequency signal representations based on tight Gabor frames. The prototype functions constituting tight frames are adaptable to diverse signal types and channel conditions. For wide-sense stationary uncorrelated scattering channels, optimized prototypes minimizing an inherent model error are presented. We obtain the optimized prototypes via convex optimization methods. Simulation results show that our prototypes perform very well unless the channel dispersions are severe in both delay and Doppler domains.

1. INTRODUCTION

In wireless communications, the usually encountered channels are doubly dispersive (DD), that is, they exhibit non-zero delay and Doppler spreads [1]. The time-frequency (TF) dispersive nature of the channel suggests that *TF analysis* techniques [2] are ideally suited tools for processing signals transmitted over DD channels. *Gabor analysis* is viewed as the branch of TF analysis which is concerned with the use of discrete coherent families [3]. Such families are obtained by applying a set of TF shifts to a given prototype (or window) function. The TF representation of a discrete-time signal can be obtained via a *Gabor transform*, which is defined as the sampled version of a short-time Fourier transform, by projecting the signal onto the set of TF shifted prototype functions. Moreover, in [4] a valuable way for the approximation of linear operators in the TF domain has been proposed, which is referred to as *Gabor multipliers*. In fact, the operators that do not involve TF shifts of large magnitude (i.e. an *underspread* channel operator) can be accurately approximated by Gabor multipliers. The accuracy of the approximation depends on the prototype functions in use and the associated lattice constants.

We are interested in using the concept of Gabor multiplier to approximate an underspread channel operator. If we multiply the coefficients of the transmitted signal in the TF representation element-wisely with the respective channel gain, the result is an approximation of the channel output in the TF domain [5]. This concept for representing DD channels can also be seen as a generalization of the frequency domain "single-tap" channel description in orthogonal frequency division multiplexing (OFDM) receivers. Furthermore, the aforementioned time and frequency shifts can be chosen in line with the coherence time and coherence bandwidth of the DD channel. In case of a fast varying channel with a small coherence time or, equivalently, a large Doppler spread, the time shift can be adjusted to small values accordingly. The scalability of the TF domain channel description in time and frequency enables the adaptation to DD channels with different delay and Doppler spreads. The proposed channel description is independent of the particular signal types (e.g., single carrier, multi carrier, spread-spectrum signals), making it suitable for *flexible radio* systems which can handle different air interfaces [6].

In [7, 8, 9] some related work on finding the optimal prototype pair of transmit pulse and matched filter for DD channels has been presented. The resulting TF well-localized pulses minimize the intersymbol/intercarrier interference caused by the time/frequency dispersion of the channel, which is advantageous over conventional OFDM signaling. A related optimization problem is addressed in this paper, however, we employ Gabor analysis for parameterizing the channel operator rather than for the signal design.

The rest of the paper is organized as follows. In Sect. 2 the TF domain channel description is discussed. An objective function for the prototype optimization is derived for wide-sense stationary uncorrelated scattering (WSSUS) channels in Sect. 3. Furthermore, a parameterization of tight Gabor frames as described in Sect. 4 is required. In Sect. 5, we discuss the optimization procedure based on semidefinite programming (SDP), and numerically computed prototype functions are presented in Sect. 6. Conclusions are drawn in Sect. 7.

Notation: We let $\mathbb{C}^{n\times n}$ denote the set of the complex $n \times n$ matrices. The set of integers is denoted as $\mathbb{Z}$, and $l_2(\mathbb{Z})$ represents the space of square-summable discrete-time sequences. The paraconjugation of a function $G(z)$ is defined by $\tilde{G}(z) = G^*(z^{-1})$, where $(\cdot)^*$ stands for complex conjugation. The imaginary unit is represented as $\jmath$. The inner product of $l_2(\mathbb{Z})$ is denoted as $\langle\cdot,\cdot\rangle$. Vectors and matrices are printed in boldface. We let $\mathrm{tr}(\mathbf{A})$ represent the trace of a matrix $\mathbf{A}$, $(\cdot)^{\mathrm{H}}$ the conjugate transpose of a matrix, and $\|\cdot\|_{\mathrm{F}}$ the Frobenius norm. We write $\mathbf{A} \geq 0$ to indicate that $\mathbf{A}$ is a Hermitian positive semidefinite matrix. The Kronecker delta function is denoted as $\delta[n]$.

2. SYSTEM MODEL

Let us consider a Gabor family of elementary functions $(g_{l,m})_{(l,m)\in\Lambda}$ with the index set $\Lambda = \mathbb{Z}\times\{0,\ldots,M-1\}$. An elementary function $g_{l,m}$ is obtained by shifting a prototype function $g \in l_2(\mathbb{Z})$ in time and frequency, i.e.,

$$g_{l,m}[n] = g[n - lN]\exp(\jmath 2\pi(n - lN)m/M) \qquad (1)$$

with N, M positive integer constants. The Gabor family $(g_{l,m})_{(l,m)\in\Lambda}$ is a *Gabor frame* for $l_2(\mathbb{Z})$, if there exist two constants $A, B > 0$ such that

$$A\,\|f\|^2 \leq \sum_{(l,m)\in\Lambda} |\langle f, g_{l,m}\rangle|^2 \leq B\,\|f\|^2$$

holds for all $f \in l_2(\mathbb{Z})$, and the frame is *tight* [10] if $A = B$. A discrete-time signal $s \in l_2(\mathbb{Z})$ can be transformed to the TF domain by the *analysis operator*

$$\mathcal{G} : s \mapsto (\langle s, g_{l,m}\rangle)_{(l,m)\in\Lambda}\,, \qquad (2)$$

where $(\langle s, g_{l,m}\rangle)_{(l,m)\in\Lambda}$ are the TF coefficients of the signal. Conversely, the *synthesis operator* $\mathcal{G}^*$ is given by

$$\mathcal{G}^* : (b_{l,m})_{(l,m)\in\Lambda} \mapsto \sum_{(l,m)\in\Lambda} b_{l,m} g_{l,m}[n]. \tag{3}$$

Note that the following discussion is based on an element density fulfilling $N/M \leq 1$, which is a necessary condition for a Gabor frame. If $(g_{l,m})_{(l,m)\in\Lambda}$ generates a normalized tight Gabor frame ($A = B = 1$), the signal can be perfectly reconstructed as $(\mathcal{G}^*(\mathcal{G}s))[n] = s[n] \;\; \forall s \in l_2(\mathbb{Z})$. In this paper, we will only consider tight Gabor frames since tight fames can be properly parameterized which allows the prototype optimization problem to be formulated in SDP form as in Sect. 5.

To analyze the signal transformation over a dispersive channel, we first define the channel operator as

$$\mathcal{H} : x[n] \mapsto y[n] = \sum_{q=0}^{\infty} c_n[q] x[n-q], \tag{4}$$

where $c_n[q]$ denotes the time-variant impulse response with n and q representing the time and delay dimensions, respectively. The channel gain over time and frequency is given by the time-variant transfer function $C_n(w) = \sum_{q=0}^{\infty} c_n[q] e^{-\jmath wq}$. In the following we represent a channel as $(h_{l,m})_{(l,m)\in\Lambda}$, where

$$h_{l,m} = C_{lN}(2\pi m/M). \tag{5}$$

Hence, given the channel input signal $x[n]$, it is straightforward to approximate the channel output signal $y[n]$ as

$$\hat{y}[n] = \sum_{(l,m)\in\Lambda} h_{l,m} \langle x, g_{l,m}\rangle g_{l,m}[n]. \tag{6}$$

In (6), the channel mapping is approximated by the concatenation of a Gabor analysis operator, an element-wise multiplication by a sequence of channel coefficients, and a Gabor synthesis operator. A linear operator of the same form as (6) is known as a Gabor multiplier [11]. The performance of the Gabor multiplier approximating the channel operator depends on the prototype function $g[n]$ and the lattice constants N and M.

The channel description (6) is similar to the frequency domain "single-tap" channel representation in OFDM receivers. In OFDM systems, the channel is viewed as a set of "flat-fading" subchannels. If we think of the DD channel having a "time-varying" frequency response, the channel coefficient $h_{l,m}$ is chosen as the channel gain at the mth subband and the lth time instant ($(lN, 2\pi m/M)$ in the TF plane). It is possible to define a TF concentrated prototype function $g[n]$ such that the energy of $g_{l,m}[n]$ is essentially confined within an area around $(lN, 2\pi m/M)$ in the TF plane. Hence, in the area around $(lN, 2\pi m/M)$ the channel can be viewed as flat, i.e., narrow-band time-invariant. This can be seen as an extension of the channel description in OFDM. Moreover, the lattice constants N and M can be chosen in line with the coherence time and frequency, respectively, of the channel.

Fig. 1 illustrates the TF domain channel description of DD channels using related filter bank theoretical notation [12]. The z-transform of the prototype function $g[n]$ is denoted as $G(z) = \sum_{n=-\infty}^{\infty} g[n] z^{-n}$. In the figure, $(\langle x, g_{l,m}\rangle)_{(l,m)\in\Lambda}$ is obtained at the output of a M channel filter bank with down-sampling factor N. The transfer function of the analysis filter bank is given by $\tilde{G}_m(z) = \tilde{G}(z \exp(\jmath 2\pi m/M)), m = 0, \ldots, M-1$. The TF coefficients $(\langle x, g_{l,m}\rangle)_{(l,m)\in\Lambda}$ of the signal $x[n]$ are multiplied element-wisely by $(h_{l,m})_{(l,m)\in\Lambda}$. Finally, the signal is transformed back to the time domain by the synthesis filter bank.

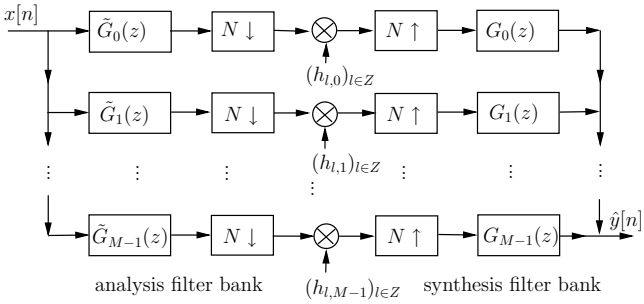

Figure 1: TF domain channel description.

The "single-tap" approximation in (6) represents the distortions of DD channels in a simple way, however, at the cost of a certain degradation in accuracy. Usually, the accuracy of the channel description directly influences the bit-error rate performance of the receiver.

3. MEAN-SQUARED ERROR ANALYSIS

To analyze how well the TF domain channel description (6) approximates the signal mapping by actual dispersive channels, we assume a WSSUS channel. The delay power spectrum is denoted as $S_\tau[q]$, where $S_\tau[q] = 0$ for $q < 0$, and the time correlation function, defined as the Fourier transform of the Doppler power spectrum, is represented as $\phi_t[n]$. The two of them are normalized such that $\sum_{q=0}^{\infty} S_\tau[q] = 1, \phi_t[0] = 1$. The second-order statistics of the channel can be represented by

$$E\left[c_u^*[m] c_n[q]\right] = \phi_t[n-u] S_\tau[m] \delta[m-q]. \tag{7}$$

Assuming the random input signal $x[n]$ with $E[x^*[n]x[m]] = \delta[n-m]$, we formulate the error from the channel description (6) as the difference between the output of the random channel $y[n] = \mathcal{H}x[n]$ and $\hat{y}[n]$ in the TF domain. The mean-squared error (MSE) per TF coefficient can be expressed as a function of the prototype $g \in l_2(\mathbb{Z})$,i.e.,

$$\epsilon_{\mathrm{MSE}_{l,m}}(g) = E\left[\left|\langle \mathcal{H}x, g_{l,m}\rangle - h_{l,m}\langle x, g_{l,m}\rangle\right|^2\right]. \tag{8}$$

Since the channel is wide-sense stationary in both l and m, $\epsilon_{\mathrm{MSE}_{l,m}}(g)$ is independent of $(l,m) \in \Lambda$. We further rewrite (8) as

$$\begin{aligned}\epsilon_{\mathrm{MSE}}(g) \;\; &= \;\; E\left[\left|\langle \mathcal{H}x, g_{l,m}\rangle\right|^2\right] + E\left[\left|h_{l,m}\langle x, g_{l,m}\rangle\right|^2\right] \\ &\quad -2E\left[\Re\left(\langle \mathcal{H}x, g_{l,m}\rangle h_{l,m}^* \langle x, g_{l,m}\rangle^*\right)\right],\end{aligned} \tag{9}$$

where $\Re(\cdot)$ denotes the real part operator. Both the input signal power and the gain of the channel are normalized to unity, and therefore $E\left[\left|\langle \mathcal{H}x, g_{l,m}\rangle\right|^2\right]$ and $E\left[\left|h_{l,m}\langle x, g_{l,m}\rangle\right|^2\right]$ equals the energy $\|g\|^2$ of the prototype, where $\|\cdot\|$ is the L^2 norm. By applying (1) and (7)

$E\left[\Re\left(\langle \mathcal{H}x, g_{l,m}\rangle\, h^*_{l,m}\,\langle x, g_{l,m}\rangle^*\right)\right]$ can be rewritten as

$$\begin{aligned}
&E\left[\Re\left(\langle \mathcal{H}x, g_{l,m}\rangle\, h^*_{l,m}\,\langle x, g_{l,m}\rangle^*\right)\right]\\
=\;& E\left[\Re\left(\sum_{n=-\infty}^{\infty}\sum_{q=-\infty}^{\infty} c_n[q]x[n-q]g^*_{l,m}[n]\right.\right.\\
&\left.\left.\cdot\sum_{k=-\infty}^{\infty} c^*_{lN}[k]e^{\jmath 2\pi mk/M}\sum_{p=-\infty}^{\infty} x^*[p]g_{l,m}[p]\right)\right]\\
=\;& E\left[\Re\left(\sum_{n=-\infty}^{\infty}\sum_{q=-\infty}^{\infty}\sum_{k=-\infty}^{\infty} c_n[q]g^*_{l,m}[n]c^*_{lN}[k]e^{\jmath 2\pi mk/M}g_{l,m}[n-q]\right)\right]\\
=\;& \Re\left[\sum_{n=-\infty}^{\infty}\sum_{q=-\infty}^{\infty}\phi_t[n-lN]S_\tau[q]g^*_{l,m}[n]g_{l,m}[n-q]e^{\jmath 2\pi mq/M}\right]\\
=\;& \Re\left[\langle \phi_t(S_\tau * g), g\rangle\right],
\end{aligned}$$

where $*$ denotes the convolution. It follows that

$$\epsilon_{\mathrm{MSE}}(g) = 2\left(\|g\|^2 - \Re\left[\langle \phi_t(S_\tau * g), g\rangle\right]\right). \tag{10}$$

We notice that the ϵ_{MSE} depends on the shape of the prototype and the second-order channel statistics. Assuming the prototype $g[n]$ has T samples and its energy equals E_g, (10) can be expressed in matrix form as

$$\epsilon_{\mathrm{MSE}}(\mathbf{g}) = 2\left(E_g - \Re\left[\mathbf{g}^{\mathrm{H}}\mathbf{B}\mathbf{g}\right]\right), \tag{11}$$

where $\mathbf{g} = [g[1], \ldots, g[T]]^{\mathrm{H}}$, and $\mathbf{B} \in \mathbb{C}^{T\times T}$ is the matrix describing the delay and Doppler domain distortions of the channel. Neglecting the constant term, we use $-2\Re\left[\mathbf{g}^{\mathrm{H}}\mathbf{B}\mathbf{g}\right]$ as the objective function for the prototype optimization later. Note that $-2\Re\left[\mathbf{g}^{\mathrm{H}}\mathbf{B}\mathbf{g}\right]$ equals $-\mathbf{g}^{\mathrm{H}}(\mathbf{B}+\mathbf{B}^{\mathrm{H}})\mathbf{g}$, and the objective function can be rewritten as $\mathbf{g}^{\mathrm{H}}\mathbf{A}\mathbf{g}$, where $\mathbf{A} = -(\mathbf{B}+\mathbf{B}^{\mathrm{H}})$ is a Hermitian matrix.

Since ϵ_{MSE} crucially depends on the chosen Gabor frame, searching for optimized prototypes minimizing ϵ_{MSE} adapted to the different channel characteristics is the next step. In [13], a general frame work is presented for parameterization of tight Gabor frames. In the following, our objective is to find a prototype function minimizing ϵ_{MSE}, which constitutes a tight Gabor frame. The optimization problem is given by

$$\hat{\mathbf{g}} = \arg\min \mathbf{g}^{\mathrm{H}}\mathbf{A}\mathbf{g}, \quad \text{s.t. } \mathbf{g} \text{ defining a tight frame.} \tag{12}$$

4. PARAMETERIZATION OF TIGHT FRAMES

In this section we briefly summarize the parameterization of tight Gabor frames presented in [13]. Let K be the least common multiple of M and N, and J and L be the two integers satisfying $JM = LN = K$. The K-component polyphase representation of $G(z)$ has the form [12]

$$G(z) = \sum_{j=0}^{K-1} z^{-j} G_j(z^K), \tag{13}$$

where

$$G_j(z) = \sum_{n=-\infty}^{\infty} g[j+nK]z^{-n}, j \in \{0, \ldots, K-1\} \tag{14}$$

is the j-th polyphase component of $G(z)$. Let $\mathbf{H}_{\mathrm{P}}(z)$ denote the $M \times N$ polyphase matrix of an analysis filter bank, the jth element of the ith row of which is defined as

$$H_{ij}(z) = \sum_{l=0}^{L-1} W_M^{-i(j+lN)} z^{-l} G_{j+lN}(z^L), \tag{15}$$

where $W_M = e^{2\pi\jmath/M}$. A filter bank is associated with a tight frame if and only if its polyphase matrix is paraunitary, i.e., $\tilde{\mathbf{H}}_{\mathrm{P}}(z)\mathbf{H}_{\mathrm{P}}(z) = c\mathbf{I}_N$, where $c = \frac{M}{N}$ represents the redundancy of the frame and $\mathbf{I}_N$ stands for the $N \times N$ identity matrix. As follows from (15), the polyphase matrix can be factored as

$$\mathbf{H}_{\mathrm{P}}(z) = \mathbf{W}_M\mathbf{D}(z), \tag{16}$$

where W_M denotes the $M \times M$ DFT matrix, and

$$\mathbf{D}(z) = [\mathbf{I}_M \cdots \mathbf{I}_M]\,\mathrm{diag}\Big(\left[G_0(z^L)\cdots G_{K-1}(z^L)\right]\Big)\begin{bmatrix}\mathbf{I}_N\\ z^{-1}\mathbf{I}_N\\ \cdots\\ z^{-(L-1)}\mathbf{I}_N\end{bmatrix}, \tag{17}$$

with $\mathrm{diag}(\mathbf{a})$ denoting the diagonal matrix whose entries of the main diagonal are the elements of the vector $\mathbf{a}$.

From the factorization in (16), the paraunitary condition of the polyphase matrix $\mathbf{H}_{\mathrm{P}}(z)$ is fulfilled when $\mathbf{D}(z)$ is paraunitary, that is, $\tilde{\mathbf{D}}(z)\mathbf{D}(z) = \frac{1}{N}\mathbf{I}_N$. Consider an example of $M = 6$, $N = 4$ and $K = 12$. According to (17),

$$\mathbf{D}(z) = \begin{bmatrix} G_0(z^3) & 0 & z^{-1}G_6(z^3) & 0\\ 0 & G_1(z^3) & 0 & z^{-1}G_7(z^3)\\ z^{-2}G_8(z^3) & 0 & G_2(z^3) & 0\\ 0 & z^{-2}G_9(z^3) & 0 & G_3(z^3)\\ z^{-1}G_4(z^3) & 0 & z^{-2}G_{10}(z^3) & 0\\ 0 & z^{-1}G_5(z^3) & 0 & z^{-2}G_{11}(z^3)\end{bmatrix}.$$

$\mathbf{D}(z)$ is paraunitary if and only if the $L \times J$ matrices

$$\mathbf{D}_0(z) = \begin{bmatrix} G_0(z) & G_6(z)\\ z^{-1}G_8(z) & G_2(z)\\ G_4(z) & G_{10}(z)\end{bmatrix} \text{ and } \mathbf{D}_1(z) = \begin{bmatrix} G_1(z) & G_7(z)\\ z^{-1}G_9(z) & G_3(z)\\ G_5(z) & G_{11}(z)\end{bmatrix}$$

are paraunitary [13].

Note that the coefficients of the polynomials in the matrices $\mathbf{D}_0(z)$ and $\mathbf{D}_1(z)$ correspond to the samples of the prototype function $g[n]$. Given the lattice constants N, M, the prototype $g[n]$ defines a tight frame if $\mathbf{D}_0(z)$ and $\mathbf{D}_1(z)$ are both paraunitary.

5. PROTOTYPE OPTIMIZATION

With the parameterization of tight Gabor frames, the tight frame constraint in (12) is equivalent to K/LJ polynomial matrices being paraunitary. In our example, $\tilde{\mathbf{D}}_0(z)\mathbf{D}_0(z) = \frac{1}{N}\mathbf{I}_J$ can be expressed as

$$\begin{cases} \tilde{G}_0(z)G_0(z) + z\tilde{G}_8(z)z^{-1}G_8(z) + \tilde{G}_4(z)G_4(z) = \frac{1}{4}\\ \tilde{G}_6(z)G_6(z) + \tilde{G}_2(z)G_2(z) + \tilde{G}_{10}(z)G_{10}(z) = \frac{1}{4}\\ \tilde{G}_0(z)G_6(z) + z\tilde{G}_8(z)G_2(z) + \tilde{G}_4(z)G_{10}(z) = 0.\end{cases} \tag{18}$$

Assume the prototype function $g[n]$ has $T = K = 12$ samples. Using (14), the first equation in (18) is rewritten as $|g[0]|^2 + |g[8]|^2 + |g[4]|^2 = \frac{1}{4}$. This can be reformulated in matrix form as $\mathbf{g}^{\mathrm{H}}\mathbf{B}_0\mathbf{g} = \frac{1}{4}$, where $\mathbf{B}_0 = \mathrm{diag}([100010001000])$. Similarly, all the remaining equations can be written in matrix form, and therefore (12) is expressed as

$$\hat{\mathbf{g}} = \arg\min_{\mathbf{g}} \mathbf{g}^{\mathrm{H}}\mathbf{A}\mathbf{g}, \quad \text{s.t. } \mathbf{g}^{\mathrm{H}}\mathbf{B}_i\mathbf{g} = d_i, i = 1, \ldots, I, \tag{19}$$

where $\mathbf{A}$ reflects the second-order channel statistics and $d_i, i = 1, \ldots, I$ are non-negative constants. The number I of the constraints in (19) depends on the order of the polynomial matrix $\mathbf{D}_t(z), t = 0, \ldots, K/(LJ) - 1$. For the case where the order of $\mathbf{D}_t(z)$ is zero (as in the example), the

number of the constraints is $K/(LJ)\cdot\left(J+\left(\begin{array}{c}J\\2\end{array}\right)\right)$. When the order of the polynomial matrices increases, the number of constraints will increase substantially. Note that if $\mathbf{X}=\mathbf{g}\mathbf{g}^{\mathrm{H}}$, $\mathbf{g}^{\mathrm{H}}\mathbf{A}\mathbf{g}=\mathrm{tr}(\mathbf{A}\mathbf{X})$. The SDP relaxation of (19) is given by

$$\hat{\mathbf{X}}=\arg\min_{\mathbf{X}}\mathrm{tr}(\mathbf{A}\mathbf{X}),\ \text{s.t.}\left\{\begin{array}{l}\mathbf{X}\geq 0\\ \mathrm{tr}(\mathbf{B}_i\mathbf{X})=d_i, i=1,\ldots,I.\end{array}\right. \tag{20}$$

It is clear that if $\hat{\mathbf{X}}=\hat{\mathbf{g}}\hat{\mathbf{g}}^{\mathrm{H}}$ is a rank-1 solution to (20), then $\hat{\mathbf{g}}$ is a solution to (19). Via the iterative interior-point algorithm [14], $\hat{\mathbf{X}}$ in (20) can be computed numerically. From now on, we use $\epsilon_{\mathrm{MSE}}(\hat{\mathbf{X}})=\left[2E_g+\mathrm{tr}(\mathbf{A}\hat{\mathbf{X}})\right]$ to represent the MSE of $\hat{\mathbf{X}}$. The rank of the resulting $\hat{\mathbf{X}}$ is larger or equal than 1 depending on $\mathbf{A}$. To obtain a rank-1 solution to (20), in the following we present a two-step procedure.

Step 1:

We first find the rank-1 matrix $\hat{\mathbf{X}}_0$ which has the least Euclidian distance to $\hat{\mathbf{X}}$. The rank-1 approximation problem can be represented as

$$\hat{\mathbf{X}}_0=\arg\min_{\mathbf{X}}\ \left\|\mathbf{X}-\hat{\mathbf{X}}\right\|_{\mathrm{F}}\quad\text{s.t.}\ \ \mathrm{rank}(\mathbf{X})=1. \tag{21}$$

Let the singular value decomposition (SVD) of matrix $\hat{\mathbf{X}}\in\mathbb{C}^{T\times T}$ be $\hat{\mathbf{X}}=\mathbf{U}\mathbf{S}\mathbf{V}^{\mathrm{H}}$ with diagonal matrix $\mathbf{S}$, and $\mathbf{U}$, $\mathbf{V}$ unitary. Then the minimum of (21) is achieved with $\hat{\mathbf{X}}_0=\mathbf{U}\hat{\mathbf{S}}_0\mathbf{V}^{\mathrm{H}}$, where $\hat{\mathbf{S}}_0$ is the matrix resulting from $\mathbf{S}$ by setting all except for the largest singular value to zero. Since $\hat{\mathbf{X}}_0$ is rank-1, a pulse $\hat{\mathbf{g}}_0$ is obtainable from $\hat{\mathbf{X}}_0=\hat{\mathbf{g}}_0\hat{\mathbf{g}}_0^{\mathrm{H}}$. However, after the rank reduction $\hat{\mathbf{X}}_0$ in general does not fulfill the constraints in (20) any more. Consequently, the resulting $\hat{\mathbf{g}}_0$ cannot construct a tight frame.

Step 2:

We then find a prototype $\hat{g}_{\mathrm{t}}\in l_2(\mathbb{Z})$ constituting a tight Gabor frame based on the resulting $\hat{g}_0\in l_2(\mathbb{Z})$ from step 1. The *Gabor frame operator* is defined by $S=\mathcal{G}^*\mathcal{G}$, and the canonical tight window can be computed as

$$\hat{g}_{\mathrm{t}}=(S^{-1/2}\hat{g}_0). \tag{22}$$

Based on a factorization of the Gabor analysis/synthesis operator, iterative algorithms to compute canonical tight frames are presented in [15]. The resulting prototype $\hat{g}_{\mathrm{t}}$ constitutes a canonical tight frame that minimizes $\|\hat{g}_{\mathrm{t}}-\hat{g}_0\|$ among all the prototypes $\hat{g}_{\mathrm{t}}$ constituting a tight Gabor frame.

6. NUMERICAL RESULTS

We assume a WSSUS channel with an exponentially decaying delay power spectrum, i.e.,

$$S_\tau[q]=(1-\exp(-1/\tau_d))\exp(-q/\tau_d),\quad q\in\{0,1,2,\ldots\}, \tag{23}$$

with τ_d representing the root mean-squared (RMS) delay spread in samples. As for the Doppler power spectrum, a Laplacian function with a two-sided exponential decay is assumed. The time correlation function, defined as the Fourier transform of the Doppler power profile, can be expressed as

$$\phi_t[p]=\frac{1}{1+2\pi^2\upsilon_D^2|p|^2},\quad p\in\mathbb{Z} \tag{24}$$

with the RMS Doppler spread υ_D relative to the sampling rate.

In the following, a sampling rate of 7.68 Msps is used (e.g. Universal Mobile Telecommunication System (UMTS) with double rate over-sampling). The lattice constants are chosen as $N=96$ and the ratio $N/M=3/4$. Since both the delay power spectrum and the time correlation function are real-valued, optimized prototypes with real values are obtained. Fig. 2 and Fig. 3 show examples of the optimized prototypes $\hat{g}_{\mathrm{t}}$. For the UMTS suburban macro cell scenario, the RMS delay spread is 170ns ($\tau_d\approx 1.3$) and the RMS Doppler spread is 100Hz ($\upsilon_D\approx 1.3\cdot 10^{-5}$) [16]. The optimized prototype obtained by SDP is shown in Fig. 2. Fig. 3 shows the optimized prototype under assumptions of larger RMS delay and Doppler spreads, that is $\tau_d=2,\upsilon_D=0.001$ (τ_d corresponds to approximately 260ns, and υ_D 7.69kHz). The waveform is more concentrated in time domain than in Fig. 2 because of the increased Doppler spread.

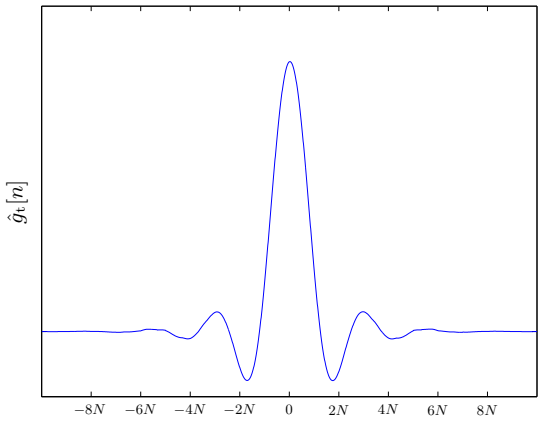

Figure 2: Optimized prototype for $\tau_d=1.3$, $\upsilon_D=1.3\cdot 10^{-5}$.

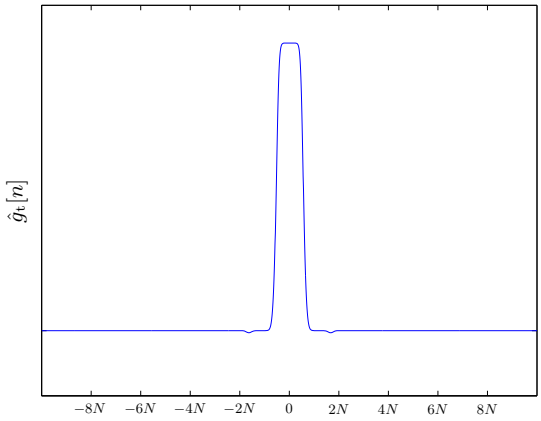

Figure 3: Optimized prototype for $\tau_d=2$, $\upsilon_D=0.001$.

Fig. 4 shows the achievable coefficient error performance by employing the optimized Gabor systems. The relative MSE per TF coefficient, given as $\epsilon_{\mathrm{MSE}}(g)/E\left[|\langle\mathcal{H}x,g_{l,m}\rangle|^2\right]=\epsilon_{\mathrm{MSE}}(g)/E_g$, are shown in dB. For increasing delay and Doppler spreads the error performance decreases as expected. In case of $\tau_d=2$ and $\upsilon_D=0.001$, the relative MSE equals -15.8 dB using the optimized prototype in Fig. 3, which indicates the MSE is approximately 2.6 percent of the signal power. The error from the channel parameterization is tolerable unless the channel dispersion is very severe.

Fig. 5 depicts a comparison of $\epsilon_{\mathrm{MSE}}(\hat{\mathbf{X}})/\mathrm{tr}(\hat{\mathbf{X}})$, $\epsilon_{\mathrm{MSE}}(\hat{g}_0)/E_{\hat{g}_0}$, $\epsilon_{\mathrm{MSE}}(\hat{g}_{\mathrm{t}})/E_{\hat{g}_{\mathrm{t}}}$, and $\epsilon_{\mathrm{MSE}}(g_{\mathrm{rect}})/E_{g_{\mathrm{rect}}}$ where g_{rect} representing the rectangular pulse, with a

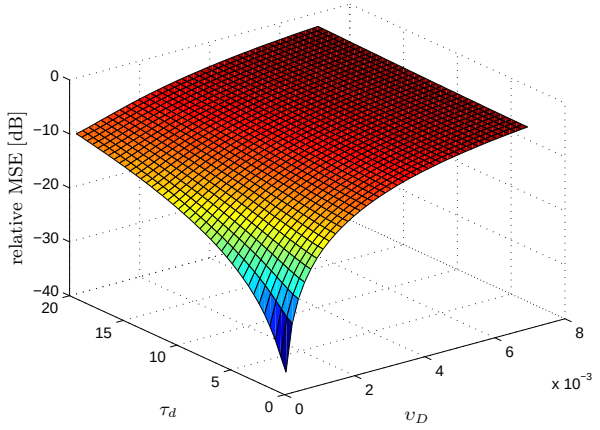

Figure 4: Relative MSE of the channel modeling in TF domain versus RMS delay and Doppler spreads.

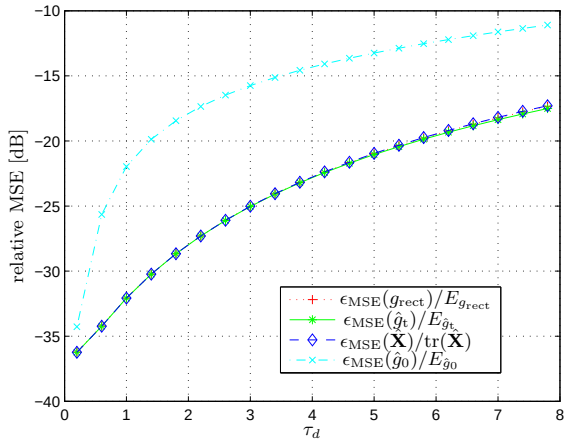

Figure 5: $\epsilon_{\mathrm{MSE}}(g_{\mathrm{rect}})/E_{g_{\mathrm{rect}}}$, $\epsilon_{\mathrm{MSE}}(\hat{g}_{\mathrm{t}})/E_{\hat{g}_{\mathrm{t}}}$, $\epsilon_{\mathrm{MSE}}(\hat{\mathbf{X}})/\mathrm{tr}(\hat{\mathbf{X}})$, and $\epsilon_{\mathrm{MSE}}(\hat{g}_0)/E_{\hat{g}_0}$ versus RMS delay spreads.

constant RMS Doppler spread $\upsilon_D = 0.0001$. From the figure, we see that when $\tau_d \leq 2.6$, the red, green and blue curves overlap perfectly, which implies the resulting $\hat{\mathbf{X}}$ of (20) is already a rank-1 matrix. The green curve shows the lowest relative MSE with $\tau_d > 2.6$, since after the rank reduction $\hat{\mathbf{g}}_0$ does not constitute a tight frame any more, which relaxes the constraint of the optimization. The cyan curve with crosses in the figure represents the relative MSE results with g representing a rectangular window of width N, which corresponds to a block DFT processing. The optimized prototype is obviously better than the rectangular one in term of the MSE performance.

7. CONCLUSIONS

We present a TF domain channel description approach, which models the behavior of DD channels via TF signal processing. By choosing TF well-localized prototypes, the proposed approach is adaptable to different channel characteristics and attains good performance for approximating signals at the output of DD channels. The optimized prototypes constituting tight Gabor frames are obtained efficiently using the SDP method. In particular, the channel description can be extended to develop techniques for channel estimation, synchronization, and signal detection. Our approach has no limitations on the signal format, making it suitable for applications in multi-mode receivers.

REFERENCES

[1] J. G. Proakis, *Digital Communications*. New York, NY: McGraw-Hill, 4th ed., 2001.

[2] K. Groechenig, *Foundations of Time-Frequency Analysis*. Boston, MA: Birkhäuser, 2001.

[3] H. G. Feichtinger and T. Strohmer, *Gabor Analysis and Algorithms: Theory and Applications*. Boston, MA: Birkhäuser, 1998.

[4] H. G. Feichtinger and K. Nowak, "A first survey of Gabor multipliers," in *Advances in Gabor Analysis*, pp. 99–128, Birkhäuser, 2002.

[5] T. Hunziker, Z. Ju, and D. Dahlhaus, "Efficient channel description in time-frequency domain with application to flexible radio," *Proc. European Signal Processing Conference (EUSIPCO-2007)*.

[6] I. Dagres, A. Zalonis, N. Dimitriou, K. Nikitopoulos, and A. Polydoros, "Flexible radio: A framework for optimized multimodal operation via dynamic signal design," *EURASIP Journal on Wireless Communications and Networking*, vol. 5, pp. 284–297, Aug. 2005.

[7] W. Kozek and A. F. Molisch, "Nonorthogonal pulseshapes for multicarrier communications in doubly dispersive channels," *IEEE Trans. Signal Processing*, vol. 16, pp. 1579–1589, Oct. 1998.

[8] T. Strohmer and S. Beaver, "Optimal OFDM design for time-frequency dispersive channels," *IEEE Trans. Commun.*, vol. 51, pp. 1111–1122, July 2003.

[9] G. Matz, D. Schafhuber, K. Grochenig, M. Hartmann, and F. Hlawatsch, "Analysis, optimization, and implementation of low-interference wireless multicarrier systems," *IEEE Trans. Commun.*, vol. 6, pp. 1921–1931, May 2007.

[10] J. M. Morris and Y. Lu, "Generalized Gabor expansions of discrete-time signals in $l_2(\mathbb{Z})$ via biorthogonal-like sequences," *IEEE Trans. Signal Processing*, vol. 44, pp. 1378–1391, June 1996.

[11] H. G. Feichtinger, M. Hampejs, and G. Kracher, "Approximation of matrices by Gabor multipliers," *IEEE Trans. Signal Processing*, vol. 11, pp. 883–886, Nov. 2004.

[12] P. P. Vaidyanathan, *Multirate Systems and Filter Banks*. Englewood Cliffs, NJ: Prentice-Hall, 1993.

[13] Z. Cvetkovic and M. Vetterli, "Tight Weyl-Heisenberg frames in $l_2(\mathbb{Z})$," *IEEE Trans. Signal Processing*, vol. 46, pp. 1256–12595, May 1998.

[14] K. C. Toh, M. J. Todd, and R. H. Tutuncu, "SDPT3 a MATLAB software package for semidefinite programming," *Optimization Methods and Software*, vol. 11, pp. 545–581, 1999.

[15] A. J. E. M. Janssen and P. L. Soendergaard, "Iterative algorithms to approximate canonical Gabor windows: Computational aspects," *Fourier Analysis and Applications*, Jan. 2006.

[16] G. Calcev, D. Chizhik, B. Gransson, S. Howard, H.Huang, A. Kogiantis, A. F. Molisch, A. Moustakas, D. Reed, and H. Xu, "A wideband spatial channel model for system-wide simulations," *IEEE Trans. Veh. Technol.*, vol. 56, pp. 389–403, Mar. 2007.